[논 문] 한국재료학회지
*Kor. J. Mater. Res.*
Vol. 18, No. 3 (2008)

DOI: 10.3740/MRSK.2008.18.3.123

# Synthesis of $SnO_2$ Microrods by the Thermal Evaporation of Sn Powders

Myung Ho Kong and Hyoun Woo Kim†

School of Materials Science and Engineering, Inha University, Incheon 402-751, Republic of Korea

(Received February 2, 2008 : Accepted March 4, 2008)

**Abstract** The production of tin oxide ($SnO_2$) microrods on iridium (Ir)-coated substrates was achieved through the thermal evaporation of Sn powders in which a sufficiently high $O_2$ partial pressure was employed. Scanning electron microscopy revealed that the product consisted of microrods with diameters that ranged from 0.9 to 40 μm. X-ray diffraction, high-resolution transmission electron microscopy, and selected area electron diffraction indicated that the microrods were $SnO_2$ with a rutile structure. As the microrod tips were free of metal particles, it was determined that the growth of $SnO_2$ microrods via the present route was dominated by a vapor-solid mechanism. The thickening of rod-like structures was related to the utilization of sufficiently high $O_2$ partial pressure during the synthesis process, whereas low $O_2$ partial pressure facilitated the production of thin rods.

**Key words** $SnO_2$, chemical synthesis, transmission electron microscopy.

## 1. Introduction

Tin dioxide ($SnO_2$), an important semiconductor with a wide band gap ($E_g$ = 3.62 eV, at room temperature), is well known for its potential applications in gas sensors,[1] transparent conducting electrodes,[2] transistors,[3] and solar cells.[4] Accordingly, various structural and morphological forms of $SnO_2$ materials have been fabricated over the past several years, including nanowires,[5-7] nanoribbons,[8-11] nanorods,[12-14] nanodiskettes,[15,16] and mesoporous powders and thin films.[17-19]

One of the most interesting and urgent challenges in materials science is the fabrication of one-dimensional (1-D) material of different sizes; smaller diameter nanorods can be utilized in the manufacture of nanoscale switching devices, whereas larger diameter rods can be useful for some optical devices and electronic applications.[20] In contrast with the extensive research that has been carried out on 1-D nanostructures as noted above, the synthesis of $SnO_2$ microrods, with larger diameters in a range of several to several tens of micrometers, has received relatively little attention. In this paper, we report on the production of $SnO_2$ microrods via a simple vapor phase deposition process. Thermal evaporation of Sn powders has been carried out at a temperature of 900°C.

In addition to nanorods, microrods are also considered promising materials for optoelectronic and sensing applications, due to their large surface-to-volume ratio. In comparison with nanorods, microrods have some notable advantages: they require a relatively broader fabrication window, and thus the fabrication cost is expected to be lower and the production yield higher.

## 2. Experimental Procedure

Thermally grown $SiO_2$ on Si(001) was employed as a starting material, onto which a layer of Ir (about 150 nm) was deposited by radio frequency magnetron sputtering. The experimental apparatus is illustrated in Fig. 1. An alumina boat containing the Sn powders (purity: 99.9%) was placed into a quartz tube in a furnace., A piece of the substrate was situated on top of the boat with the Ir-coated side oriented downwards. The powder-to-substrate distance was approximately 10 mm. Before evaporation, the tube was evacuated to 0.01 Torr by a mechanical pump. During the experiment, a constant pressure of 1 Torr with an oxygen ($O_2$) flow was maintained, where the $O_2$ partial pressure was about 21%. The temperature near the substrate was held at roughly 900°C for 2 hours. After evaporation, the substrate was cooled down and subsequently removed from the furnace for structural characterization. A white layer was observed on the surface of the substrate.

The structural properties of the as-grown products were investigated by grazing angle X-ray diffraction (XRD: $CuK\alpha_1$ radiation) (Philips X'pert MRD) with an incidence angle

†Corresponding author
E-Mail : hwkim@inha.ac.kr (H. W. Kim)

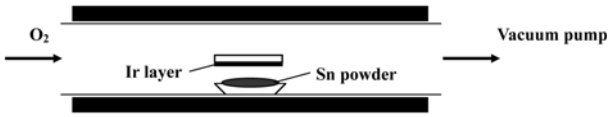


**Fig. 1.** Schematic illustration of the apparatus used in this work.

of 0.5°, scanning electron microscopy (SEM, Hitachi S-4200), and transmission electron microscopy (TEM, Philips CM-200) with energy-dispersive x-ray spectroscopy (EDS) installed. TEM specimens were prepared by sonication in acetone, and subsequently dropping them onto a holey carbon film supported on a copper grid.

## 3. Results and discussion

The XRD pattern shown in Fig. 2 reveals the overall crystal structure of the product on the Ir-coated substrate. Miller indices are indicated on each diffraction peak. The diffaction peaks of (110), (101), (200), (211), (220), (002), (310), (112), (301), (202), and (321) correspond to the tetragonal rutile structure of $SnO_2$ with lattice constants of a = 4.734Å and c = 3.185Å (JCPDS File No. 41-1445). No impurities, such as unreacted Sn or other tin oxides, were detected. In the XRD measurements, the angle of the incident beam to the substrate surface was about 0.5°, and the detector was rotated to scan the samples. Therefore, it was surmised that the peaks mainly originate from the products.

Fig. 3a is a typical plan-view SEM image of the products, showing an agglomeration of solid 1-D structures over a large area. Close examination reveals that the cross section of the 1-D structures is close to rectangular-or polygonal-shaped. The rods have an almost straight-line morphology along the length direction as well as smooth surfaces, with no nanoparticles at their tips. Fig. 3b is a SEM image presenting a side view of the products on the substrate surface, showing random growth directions of the 1-D structures. Statistical analysis of numerous SEM images shows that the 1-D structures have diameters ranging from 0.9 to 40 μm and lengths up to several hundreds of micrometers.

Fig. 4a shows a TEM image of two microrods, revealing that the rods have an almost straight-line morphology. No particles are observed at the flat tip ends of the microrods. The EDS analysis indicated that the synthesized products consist of only Sn and O elements, regardless of the

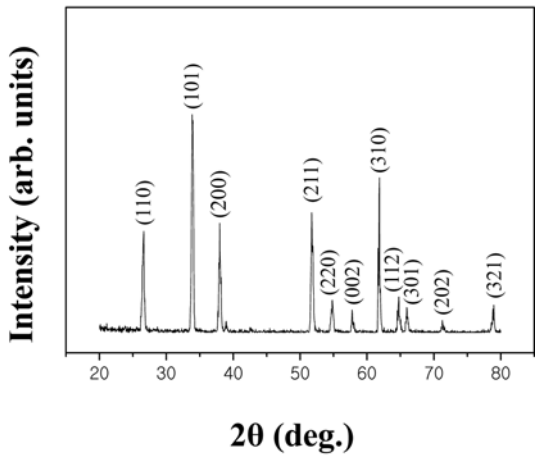


**Fig. 2.** XRD pattern recorded from the products on an Ir-coated substrate.


(a)

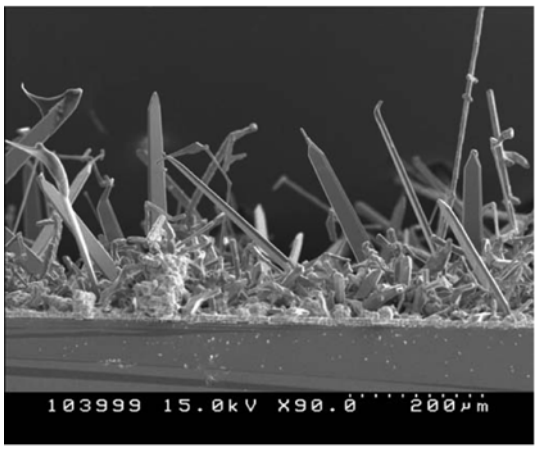


(b)

**Fig. 3.** (a) Plan-view and (b) Side view SEM image of the products.

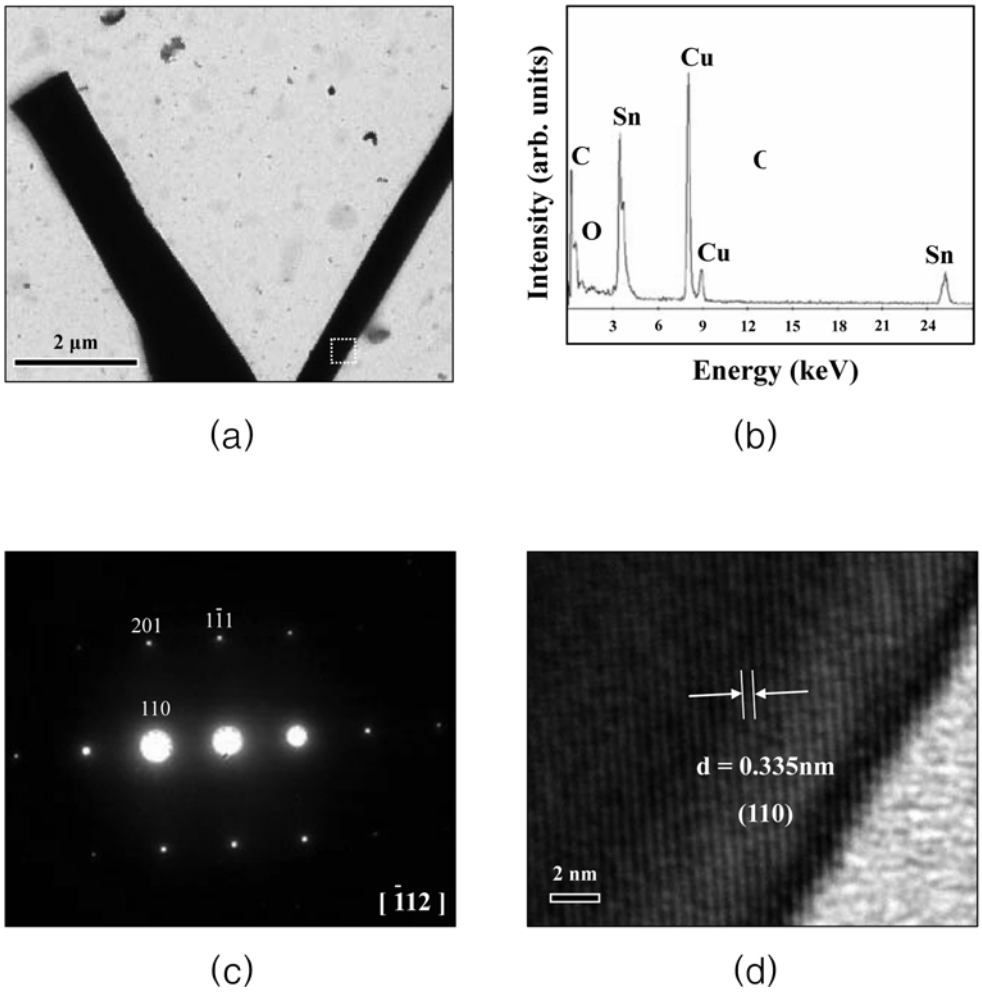


**Fig. 4.** (a) TEM image of two mocrorods. (b) EDS spectrum of a single $SnO_2$ microrod. (c) Corresponding SAED pattern recorded along the [$\bar{1}$12] zone axis. (d) HRTEM image of the area marked in (a).

location in the microrod from the stem to the end. The associated EDS spectrum, recorded from a single microrod, is shown in Fig. 4b. The C- and Cu-related signals, respectively, are due to contamination of C during preparation of TEM specimens as well as to the presence of Cu grids.

Fig. 4c shows a selected area electron diffraction (SAED) pattern taken from a microrod with a diameter of approximately 0.94 μm in Fig. 4a, recorded perpendicular to the microrod long axis. The SAED pattern can be indexed to the [$\bar{1}$12] zone axis of crystalline $SnO_2$. The SAED pattern also indicates that at least a portion of the $SnO_2$ microrod is single crystalline, being consistent with the above XRD measurement. Fig. 4d is a high resolution TEM (HRTEM) image corresponding to the area marked in Fig. 4a, revealing good crystallinity. The interplanar spacing is approximately 0.335 nm, corresponding to the (110) plane of rutile $SnO_2$.

Our previous experiments on the growth of $SnO_2$ 1D nanostructrures revealed that the $O_2$ partial pressure determines the morphology of the final nanostructures.[22] A statistical analysis of many SEM images indicated that the diameters of the $SnO_2$ 1D nanomaterials produced with $O_2$ partial pressures of 3, 4, and 6%, respectively, were in a range of 50-500 nm, 150 nm-1.8 μm, and 400 nm-6.3 μm. These results indicate that the average width or diameter of the structures increases overall with increasing $O_2$ partial pressure in a range of 3-6%.[22]

In the present work, we employed a very high $O_2$ partial pressure (about 21%) and produced very thick 1D structures with diameters in a range of 0.9-40 μm, which are in agreement with previous results. Since SEM images and EDS measurement indicate that the microrod tips are free of metal particles, it was surmised that the growth of

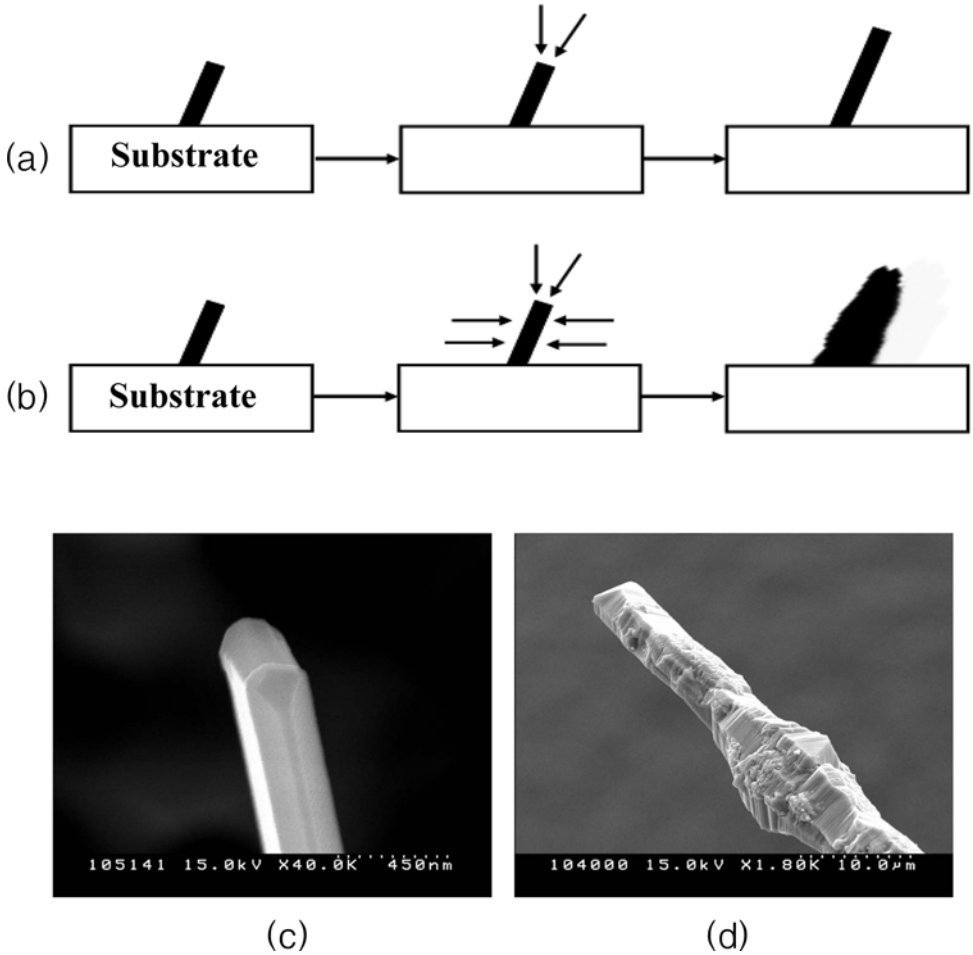


**Fig. 5.** Schematic illustration of the product formation with (a) low and (b) high $O_2$ partial pressures. Typical SEM images of the 1D structure grown on Ir-coated substrates with an $O_2$ partial pressure of (c) 6% and (d) 21%.

$SnO_2$ microrods via the present route is dominated by a vapor-solid mechanism, in which the Sn atoms from Sn powders react with O atoms to form metastable SnO, subsequently decomposing into $SnO_2$ and Sn.[21] The precipitated solid $SnO_2$ acts as the nuclei of the $SnO_2$ microrods.

In a vapor-phase reaction system, the two-dimensional (2D) nucleation probability on the surface of a whisker is approximately proportional to exp (-A /ln$\alpha$), where A is a positive constant and $\alpha$ the supersaturation ratio, under the hypothesis that the parameters such as temperature and surface energy are invariant.[23] The supersaturation ratio is defined by $\alpha = p/p_0$, with p being the actual vapor pressure and $p_0$ the equilibrium vapor pressure. The high-$O_2$ partial pressure-process induces high actual vapor pressure (p) and thus a high oxygen supersaturation ratio, increasing the 2D nucleation probability on the surface of a whisker. This facilitates the 2D growth and thus the formation of thick 1D structures (Fig. 1d). On the other hand, a synthesis process with a low $O_2$ partial pressure brings about low $O_2$ supersaturation and thus the suppression of 2D growth, ultimately resulting in the generation of thin 1D structures. Schematic outlines for the formation of a 1D structure under low and high $O_2$ partial pressure are shown in Figs. 5 and 5b, respectively. Figs. 5c and 5d present SEM images representing typical 1D structures grown on Ir-coated substrates with an $O_2$ partial pressure of 6% and 21%, respectively.

## 4. Conclusions

In summary, we successfully synthesized crystalline microrods on an Ir-coated substrate via a thermal evaporation method of heating Sn powders in the presence of an $O_2$ flow. The obtained $SnO_2$ microrods, with diameters in a range of 0.9-40 μm and lengths up to several hundreds of

micrometers, are tetragonal rutile structures. We suggest that the thickening of these rod-like structures is related to the utilization of sufficiently high $O_2$ partial pressure during the synthesis process, which leads to $O_2$ super-saturation and thus higher 2D nucleation probability on the surfaces of 1D structures.

## Acknowledgements

This work was supported by Inha University Research Grant. This work was supported by a Korea Research Foundation Grant funded by the Korean Government (MOEHRD) (KRF-2007-521-D00216). The main calculations were performed by the supercomputing resources of the Korea Institute of Science and Technology Information (KISTI).

## References

1. E. R. Leite, I. T. Weber, E. Longo and J. A. Varela, Adv. Mater., **12**, 966 (2000).
2. Y. S. He, J. C. Campbell, R. C. Murphy, M. F. Arendt and J. S. Swinnea, J. Mater. Res., **8**, 3131 (1993).
3. G. Sberveglieri, Sensor Actuators, **B6**, 64 (1992).
4. S. Ferrere, A. Zaban and B. A. Gsegg, J. Phys. Chem., **B101**, 4490 (1997).
5. M. Zhang, G. Li, X. Zhang, S. Huang, Y. Lei and L. Zhang, Chem. Mater., **13**, 3859 (2001).
6. R.-Q. Zhang, Y. Lifshitz and S.-T. Lee, Adv. Mater., **14**, 1029 (2003).
7. A. Kolmakov, Y. Zhang, G. Cheng and M. Moskovits, Adv. Mater., **15**, 997 (2003).
8. Z. R. Dai, Z. W. Pan and Z. L. Wang, Solid State Commun., **118**, 351 (2001).
9. Z. L. Wang and Z. Pan, Adv. Mater., **14**, 1029 (2002).
10. J. Q. Hu, X. L. Ma, N. G. Shang, Z. Y. Xie, N. B. Wong, C. S. Lee and S. T. Lee, J. Phys. Chem. **B106**, 3823 (2002).
11. X. S. Peng, L. D. Zhang, G. W. Meng, Y. T. Tian, Y. Lin, B. Y. Geng and S. H. Sun, J. Appl. Phys., **93**, 1760 (2003).
12. Y. Liu, C. Zheng, W. Wang, C. Yin and G. Wang, Adv. Mater., **13**, 1883 (2001).
13. C. Xu, G. Xu, Y. Liu, X. Zhao and G. Wang, Scr. Mater., **46**, 789 (2002).
14. D.-F. Zhang, L.-D. Sun, J.-L. Yin and C.-H. Yan, Adv. Mater., **15**, 1022 (2003).
15. Z. R. Dai, Z. W. Pan and Z. L. Wang, J. Am. Chem. Soc., **124**, 8673 (2002).
16. Z. L. Wang, Adv. Mater., **15**, 432 (2003).
17. Z. Zhong, Y. Yin, B. Gates and Y. Xia, Adv. Mater., **12**, 206 (2000).
18. D. N. Srivastava, S. Chappel, O. Palchik, A. Zaban and A. Gedanken, Langmuir, **18**, 4160 (2002).
19. H. Miyata, M. Itoh, M. Watanabe and T. Noma, Chem. Mater., **15**, 1334 (2003).
20. C. K. Xu, X. L. Zhao, S. Liu and G. H. Wang, Solid State Commun., **125**, 301 (2003).
21. J. Q. Hu, X. L. Ma, N. G. Shang, Z. Y. Xie, N. B. Wong, C. S. Lee and S. T. Lee, J. Phys. Chem., **B106**, 3823 (2002).
22. H. W. Kim and S. H. Shim, J. Korean Phys. Soc., **47**, 516 (2005).
23. Z. R. Dai, Z. W. Pan and Z. L. Wang, Adv. Funct. Mater., **13**, 9 (2003).